

X-ray Astronomy



Overview

- Introduction
 - Key milestones in X-ray observing
 - X-ray emission mechanisms
- X-ray optics
 - Grazing incidence
 - Wolter 1 configuration
- X-ray photon detectors
 - Gas-filled detectors
 - Multi-channel plates
 - CCDs
- Signal-to-noise ratio

Major X-ray Observatories

Satellite	Period	Instruments	Resolution	Comment
Uhuru	1970-1973	2 proportional counters	0.5 deg, 5 deg	First all sky survey; discovered X-ray emission from galaxy clusters
HEAO-1	1977-1979	4 instruments	Best 1 deg	Discovered X-ray background
Einstein	1978-1981	IPC, HRI, Spectrograph	1 arcmin	First imaging X-ray telescope; discovered X-ray jets
ROSAT	1990-1999	PSPC, HRI	15 arcsec	All-sky survey (RASS); 150,000 sources
ASCA	1993-2001	GIS, SIS	30 arcsec	First X-ray CCD; Great Spectra!
Chandra	1999-	HRC, ACIS, 2 gratings	< 1 arcsec	The HST of X-ray observatories!
XMM-Newton	1999-	CCD, grating	6 arcsec	Large collecting area- 1500 cm ² at 1 keV

ROSAT All-Sky Survey (RASS)

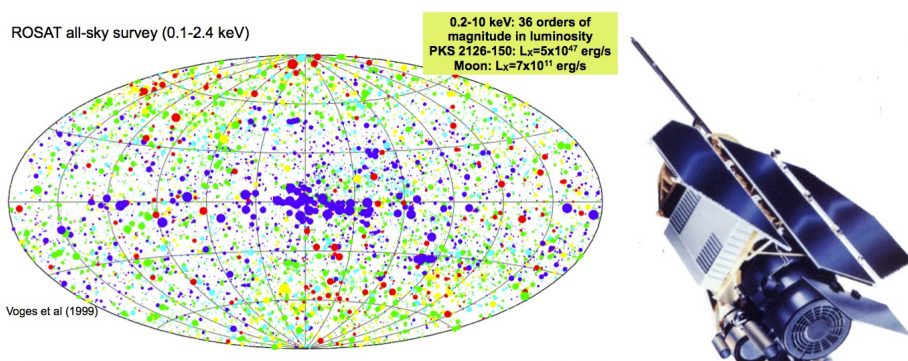
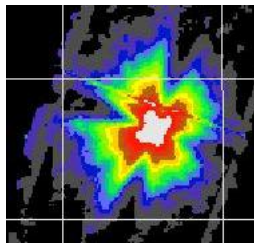


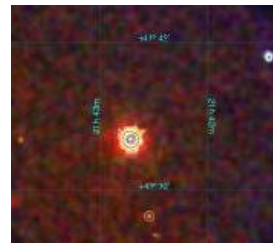
Fig. 5. Aitoff projection of the distribution of all RBSC sources obtained in the ROSAT All-Sky Survey observations until August 13, 1991 in galactic coordinates. The size of the symbols scales with the logarithm of the count-rate and the colours represent 5 intervals of the hardness ratio HR1: red ($-1 \leq HR1 < -0.6$); yellow ($-0.6 \leq HR1 < -0.2$); green ($-0.2 \leq HR1 < 0.2$); blue ($0.2 \leq HR1 < 0.6$) and violet ($0.6 \leq HR1 \leq 1.0$).

X-ray image quality over the years

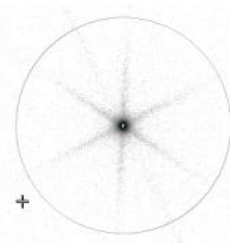
Same star: SS Cyg



ASCA 1993
resolution 75"
The first satellite to use
CCD's in space, and so
the detectors (and not the
mirrors) were the priority
of the mission



ROSAT 1990
resolution 10"
Superb spatial resolution,
albeit at lower X-ray
energies (only up to 2
keV)



Chandra 2000
resolution 0.3"
Latest generation,
designed specifically
for high quality imaging

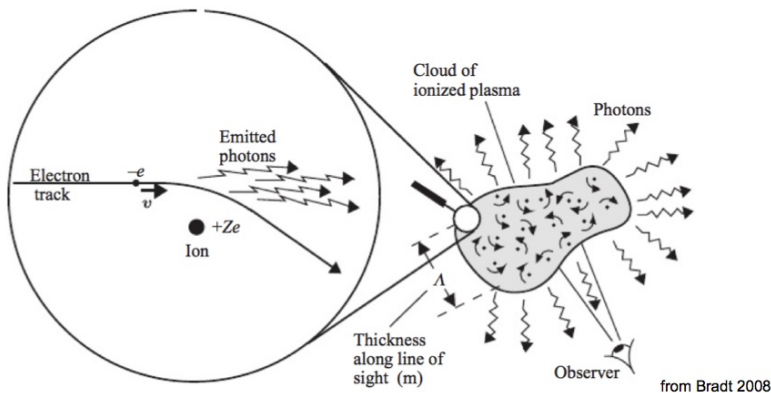
Thermal and Non-thermal Emission

- Electromagnetic radiation is emitted by charged particles when they accelerate
- **Thermal** emission caused by acceleration of charged particles due to the temperature of the emitting body
 - black body radiation
 - free-free emission
 - line emission
- **Non-thermal** emission caused by acceleration of charged particles not due to the temperature of the emitting body
 - synchrotron emission
 - masers

Bremsstrahlung – “free-free” emission

consider a hot optically thin plasma transparent to its own radiation in thermal equilibrium

Thermal Bremsstrahlung by electrons (Maxwellian velocity distribution)

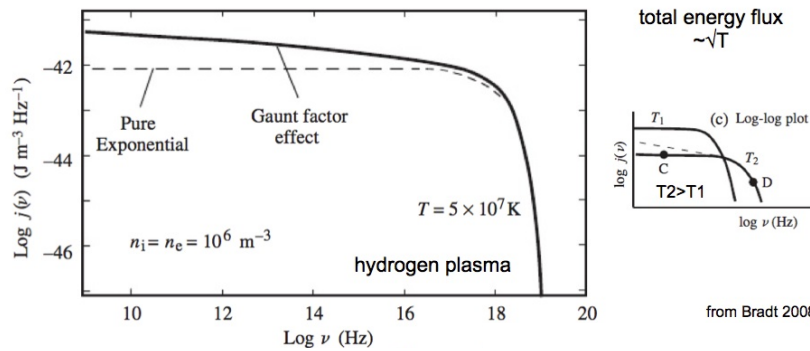


Bremsstrahlung – “free-free” emission

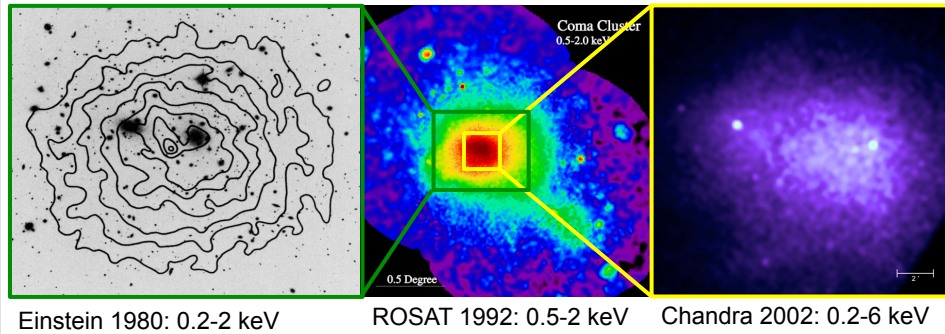
consider a hot optically thin plasma transparent to its own radiation in thermal equilibrium

Thermal Bremsstrahlung by electrons (Maxwellian velocity distribution)

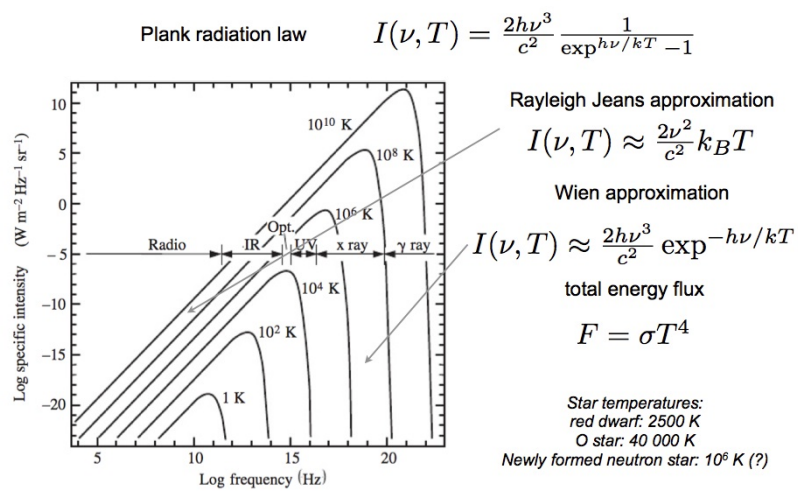
$$\frac{dW}{dV dt d\nu} = \frac{2^5 \pi e^6}{3c^3 m} \left(\frac{2\pi}{3k_B m} \right)^{1/2} Z^2 n_e n_{ion} T^{-1/2} e^{-(h\nu/k_B T)} \bar{g}_{ff}$$



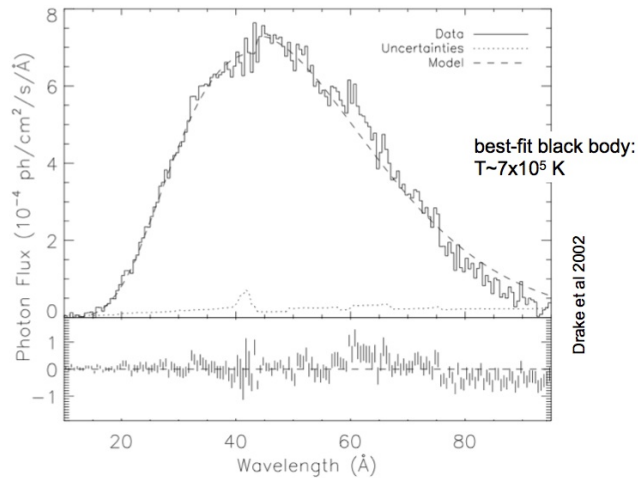
X-ray Imaging of Free-free emission Coma Cluster over the years



Black-body Radiation

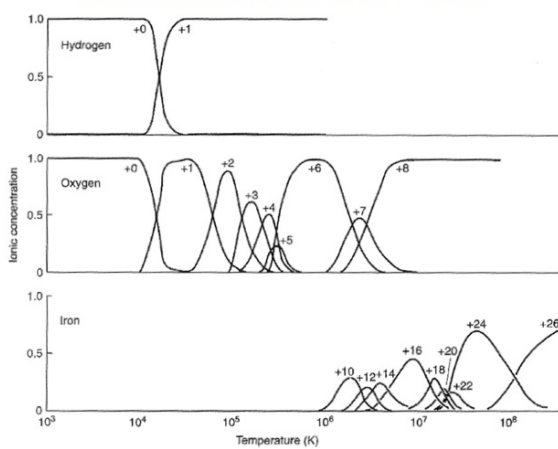


RXJ1856.5-3754 – isolated neutron star



X-ray line emission – bound-bound emission

line emission: heavy elements not completely ionized
(except at very high temperatures $>5 \times 10^7$ K)



Seward & Charles Fig 2.2

Example X-ray Spectrum

L108

J. R. Peterson et al.: X-ray imaging-spectroscopy of Abell 1835

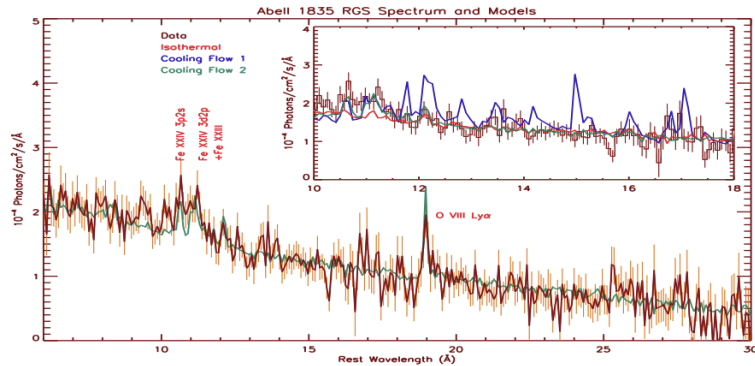


Fig. 4. RGS spectrum of Abell 1835 and three models folded through the instrument Monte Carlo. The same corrections and data selection cuts have been applied to the data and the simulated photons. The red model is an isothermal 8.2 keV model. The blue model has an hot ambient 8.2 keV component and an isobaric cooling flow component. The green model is the same as the blue model but does not have emission below 2.7 keV. The details of each model are described in the text. The spectrum is corrected for redshift, exposure, and effective area

Photon Energy

Optical photon at $\lambda = 500$ nm:

$$E = h\nu = h \frac{c}{\lambda} = 6.6 \times 10^{-34} Js \times \frac{3 \times 10^8 ms^{-1}}{500 \times 10^{-9} m} = 4 \times 10^{-19} J \approx 2.5 eV$$

Radio “photons” at $\lambda = 21$ cm:

$$E = h\nu = h \frac{c}{\lambda} = 6.6 \times 10^{-34} Js \times \frac{3 \times 10^8 ms^{-1}}{0.21m} = 3.8 \times 10^{-25} J \approx 2.4 \times 10^{-6} eV$$

Radio waves detected via induced oscillating electric current

X-ray photons at $\lambda = 0.25$ nm:

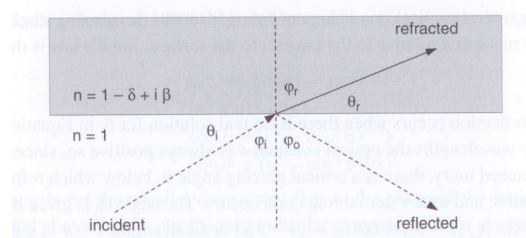
$$E = h\nu = h \frac{c}{\lambda} = 6.6 \times 10^{-34} Js \times \frac{3 \times 10^8 ms^{-1}}{0.25 \times 10^{-9} m} = 7.9 \times 10^{-16} J \approx 5 keV$$

X-rays collected with grazing incidence mirrors

14

Total External Reflection

- In general:
 - X-rays penetrate materials
 - X-rays are absorbed if material is thick enough
- At grazing incidence:
 - X-ray photons interact with ensemble of surface electrons
 - X-rays are scattered coherently such that $\phi_i = \phi_o$
 - Total external reflection occurs



Total External Reflection

Consider a medium of refractive index n :

At X-ray energies:

If medium is conducting then the refracted beam decays exponentially:

Consider X-ray photons of energy E incident on the medium. Snell's law gives:

Re-write in terms of the grazing angle:

The angle of refraction will reach zero at the critical grazing angle incidence:

For small angles: $1 - \theta_c^2 / 2 \approx (1 - \delta)$

$$n = 1 - \delta + i\beta$$

$$0 < \delta \ll 1 \quad \beta \ll 1$$

$$\beta > 0$$

$$\sin \phi_r = \sin \phi_i / (1 - \delta)$$

$$\cos \theta_r = \cos \theta_i / (1 - \delta)$$

$$\cos \theta_c = (1 - \delta)$$

$$\theta_c \approx \sqrt{2\delta}$$

Total External Reflection

Critical grazing angle of incidence at reflection occurs: $\theta_c \approx \sqrt{2\delta}$

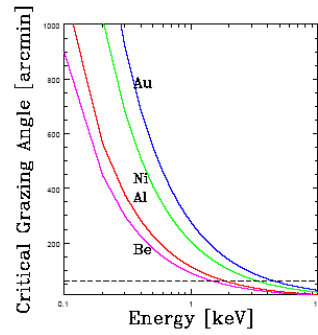
At photon energies, E, the optical constant δ is given by:

$$\delta = r_e \left(\frac{hc}{E} \right)^2 \frac{N_e}{2\pi}$$

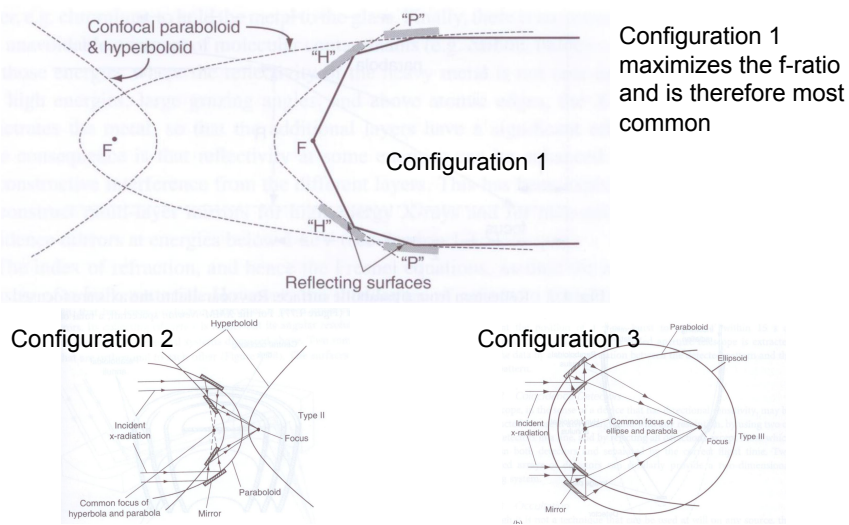
r_e is classical radius of the electron, and N_e is the number density of electrons

Critical grazing angle of incidence can therefore be written in terms of atomic number and photon energy:

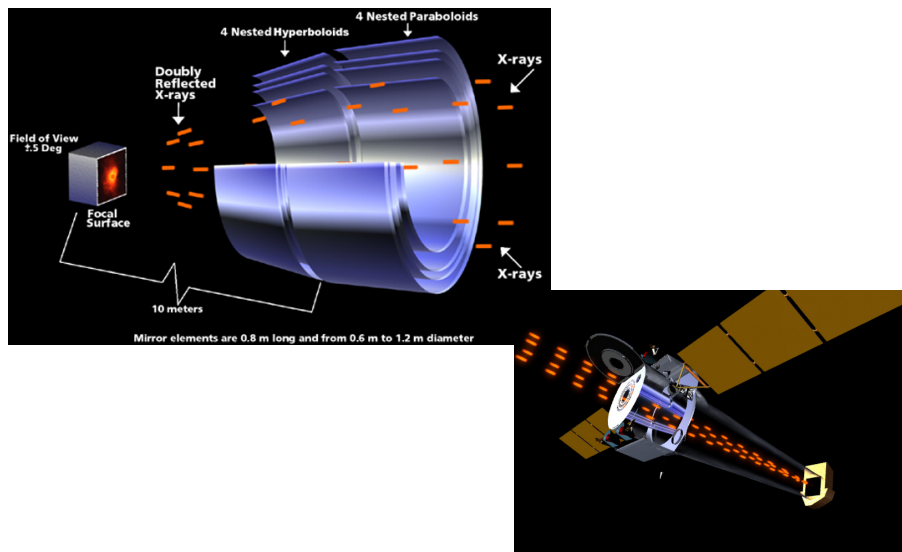
$$\theta_c \propto \frac{\sqrt{Z}}{E}$$



Wolter's Configurations



Nested Mirrors: Chandra



Nested Mirrors: XMM-Newton



Focal length =	7500mm
Number of mirrors =	58
Outer mirror radius =	350mm
Inner mirror radius =	153mm
Axial mirror length =	600mm
Outer mirror thickness =	1.07mm
Inner mirror thickness =	0.47mm
Minimum packing distance =	1mm
Mirror substrate =	Nickel
Reflective coating =	Gold

} Why?

Light Collecting Power

Light collecting power of optical telescopes depends on diameter of primary mirror:

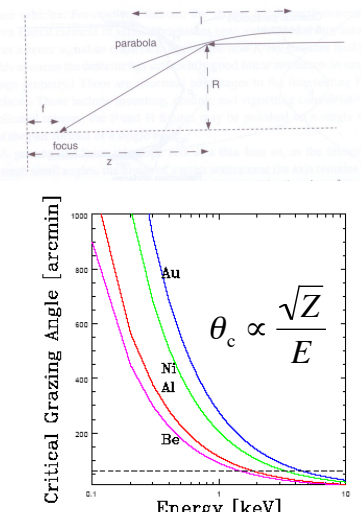
$$LCP \propto A = \pi \left(\frac{D}{2} \right)^2$$

Light collecting power of X-ray telescopes also depends on grazing angle

$$LCP \propto A \sin \theta_c \approx 2\pi R l / \theta_c \propto \frac{\sqrt{Z}}{E}$$

Materials with high atomic number are therefore used for X-ray mirrors, especially at $\sim 1\text{-}10\text{ keV}$

Chandra and XMM mirrors are coated with Iridium and Gold respectively – what are their atomic numbers?



Light Collecting Power

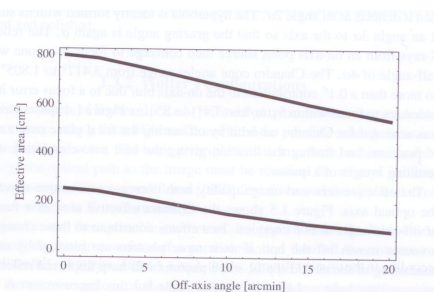


Fig. 1.5 The change in effective collecting area with off-axis angle, at 1.5 keV (top curve) and 6.4 keV (bottom curve). At higher energies, the relative area decrease is greater

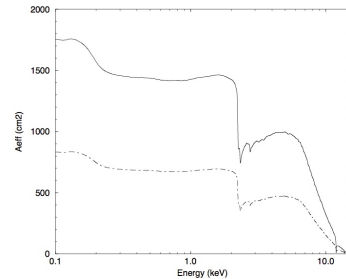
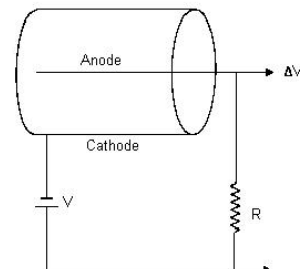


Fig. 2. On-axis effective area of the XMM telescopes without (solid line) and with (dot-dashed line) Reflection Grating Assembly (RGA).

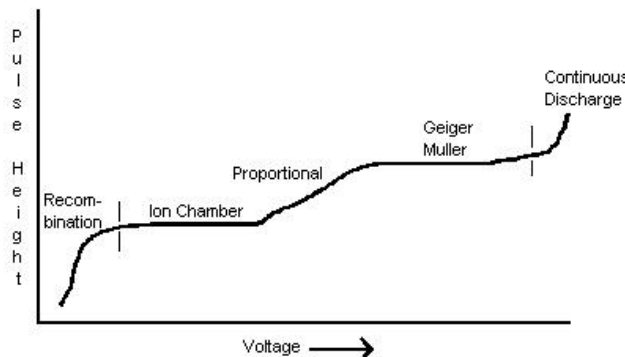
At 6keV the light collecting power of Chandra and XMM is equivalent to optical telescope primary mirror diameters of D=8cm and D=12cm respectively!

Gas-Filled Detectors

- Incident X-rays interact with chamber walls or gas particles and produces electron/ion pairs
- Ions are attracted towards negatively charged cathode
- Electrons are attracted towards positively charged anode
- Charge accumulates on anode, causing a voltage change in the circuit
- Change in voltage is referred to as a pulse



Output pulse for a discharge tube



Recombination region:

- Electric force on electrons is weak
- Re-combination is common
- Pulse depends rate of recombination

Ion chamber region:

- Recombination is negligible
- ~All electrons reach the anode
- Pulse independent of voltage

Proportional region:

- Ions strongly accelerated
- Secondary ionizations common
- Pulse height proportional to photon energy
- "Gas multiplication"

Geiger Mueller region:

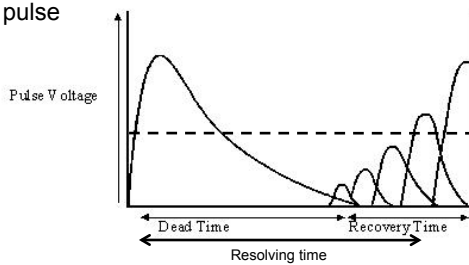
- Secondary ionizations saturate
- Pulse height independent of voltage and photon energy

Proportional counter

- Operates in the proportional region
- Gas multiplication increases number of ions produced by 10^4
- Each X-ray photon therefore produces $\sim 10^4$ electrons
- Output from a proportional counter is a series of pulses
- Pulses are counted by a counting circuit
- “Resolving time” is generally $< 10^{-3}$ seconds
- High pulse rates can be counted

Resolving Time

- Defined as the minimum amount of time separating two events that are recorded as two separate pulses
- Depends on the following factors:
 - **Dead time** – length of time between formation of an output signal (pulse) and detector conditions being able to produce another output signal
 - **Recovery time** – length of time for detector to recover from an ionization event and return to its original condition
 - **Discriminator level** – voltage level at which electronic circuit counts a pulse



What are the consequences of dead time for detection of X-ray photons?

How might these consequences be overcome?

ROSAT PSPC

Position sensitive proportional counter

- Number of electrons released proportional to photon energy: $N = E/w$
- w is mean energy required to release a secondary electron
- $w = 26.2 \text{ eV}$ for argon, 21.5 eV for xenon
- Presence and position of electron cloud measured by a 2D grid of electrodes

QE of Proportional Counters

Consider a photon incident on the window of a proportional counter (e.g. PSPC).

Quantum efficiency of the device depends on the probability that the photon passes through the window and interacts with a gas particle:

$$P = e^{-\tau_w} (1 - e^{-\tau_g})$$

Where τ_w and τ_g are the optical depths of the window and gas respectively:

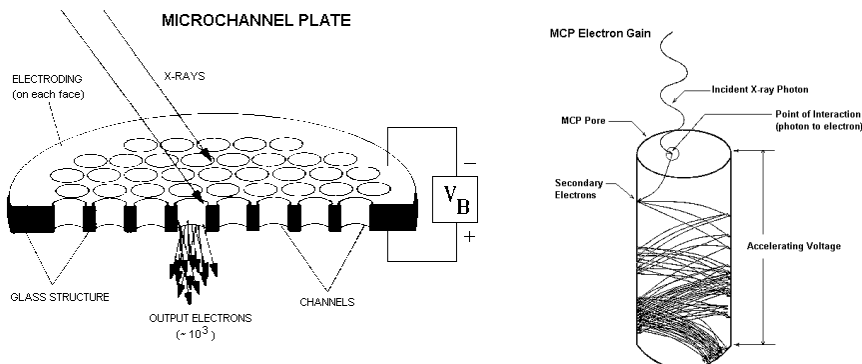
$$\tau_w = \rho_w \mu_w x_w \quad \tau_g = \rho_g \mu_g x_g$$

What else does QE depend on?

Fig. 2.1 Mass attenuation coefficient for argon (Hubbell and Seltzer, 2004)

Microchannel Plates

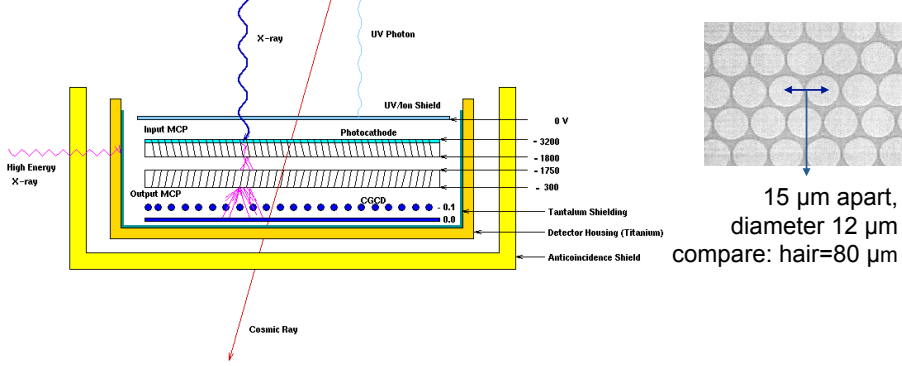
- A typical MCP has 10^7 closely packed channels each of diameter $10\mu\text{m}$
- A single x-ray photon interacting in a channel of the MCP produces a charge pulse of about 1000 electrons that emerge from the rear of the plate.
- Spatial pattern of electron pulses emerging from plate matches the pattern (image) of x-rays incident on the front surface



Example:

Chandra High Resolution Camera

- Each channel or pore of the MCP is coated with CsI/KBr or similar photo-emitting material
- A UV/Ion shield consisting of Lexan or aluminized polyimide stops low energy ions and electrons



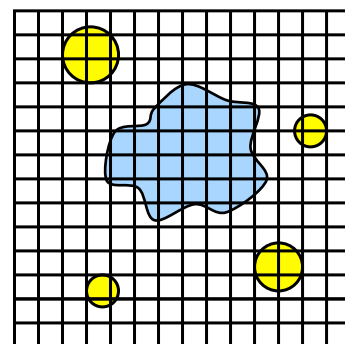
Micro Channel Plates

- Advantages:
 - High spatial resolution
 - Good QE at low photon energy (soft X-ray and UV)
 - No consumables (e.g. gas, coolant)
- Disadvantage:
 - Pulse height is a very weak function of photon energy
- Questions:
 - Why is pulse height a weak function of photon energy?
 - Which optical detector do MCPs remind of?

Reminder #1

CCDs: Basic Idea

- Solid state detector
- Typically 1k x 1k light sensitive elements (pixels)
- Each pixel about 10-20um square
- Pixels electrically insulated from each other
- Charge accumulates in each pixel
- Amount of charge proportional to intensity of light
- Charge distribution is the same as the light distribution

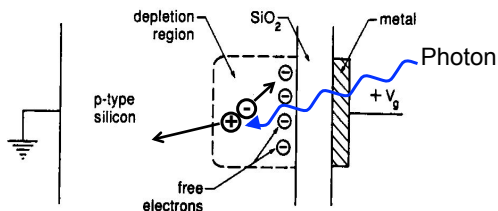


What are the key parameters that quantify CCD performance?

Reminder #2

CCDs: Structure of a CCD pixel

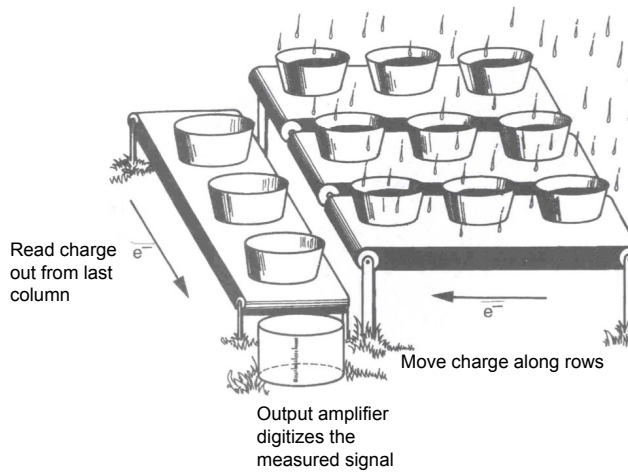
Metal Oxide Semi-conductor (MOS) Capacitor



- Metal electrode:
 - $V_g \sim +10\text{V}$
 - Insulated from p-type Si substrate by layer of SiO_2 ($\sim 0.1\mu\text{m}$ thick)
- Repels holes causing a –vely charged depletion region
- Incoming photons of energy $< E_g$ create electron-hole pairs in Si substrate
- Holes diffuse away from metal electrode
- Electrons diffuse towards metal electrode and stored in depletion region

Reminder #3

CCDs: Reading out a CCD



Physically how is charge transferred from pixel to pixel?

Silicon as a detector of X-rays

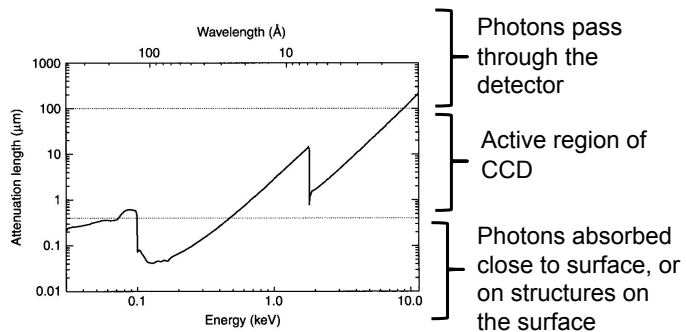


Fig. 3.1 The attenuation length or mean absorption depth of an X-ray photon in silicon as a function of the photon energy and wavelength. The horizontal dotted lines indicate typical active regions in an X-ray CCD which correspond to an energy range of about a few hundred eV to 10 keV. The best X-ray sensitivity will be in this range

Silicon as a detector of X-rays

Each X-ray photon produces many electron-hole pairs:

$$N_e = E_X / w$$

Photon energy Ionization energy

What is a typical value of N_e ?

An X-ray CCD image can be used to measure photon energy (crude spectroscopy). Why is this?

How does the energy resolution of an X-ray CCD image depend on N_e ?

Reading out an X-ray CCD

Output data rate ~10Mbits/sec/CCD!

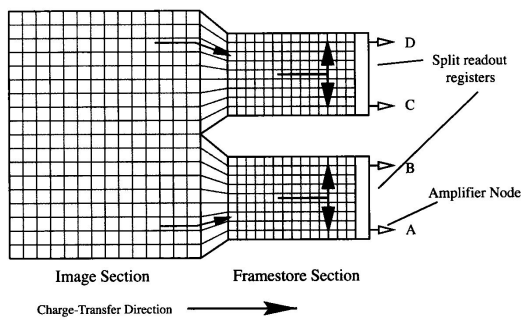


Fig. 3.4 Schematic representation of an ACIS CCD showing the frame-transfer architecture and the four readout nodes. The schematic is rotated such that columns are in the horizontal direction and rows in the vertical. Source: Science Instrument Calibration Report for the AXAF CCD Imaging Spectrometer (ACIS)

X-ray CCDs generally operate in photon counting mode

Requirement for <=1 photon per pixel per "frame time" (typically a few seconds)

After read-out from framestore the data are analyzed on-board to generate an event file for transmission back to Earth

Quantum Efficiency

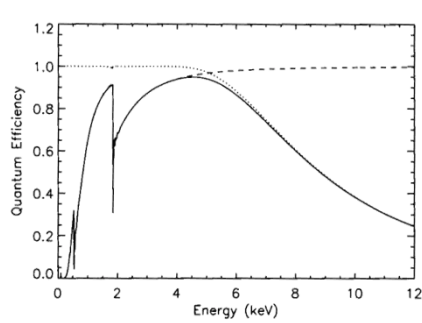


Fig. 3.7 The quantum efficiency of a CCD (solid line) is the product of the transmission probability through various dead layers (dashed line) and probability of absorption in the depletion region (dotted line)

Transmission of photons through "dead" layers (gates, insulators, etc.) of absorption co-efficients μ_i and thicknesses t_i :

$$T = \prod_i e^{-\mu_i t_i}$$

Absorption of photons in the depletion region (Silicon) of absorption co-efficient μ_{Si} thickness d:

$$A = 1 - e^{-\mu_{Si} d}$$

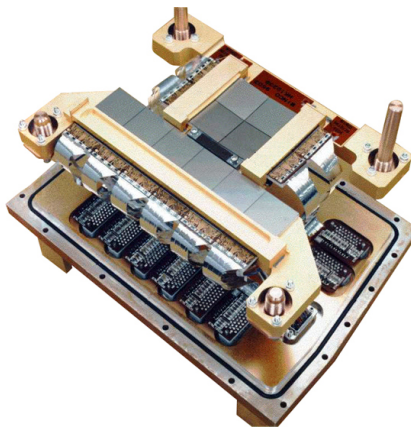
Quantum efficiency:

$$QE = TA = (1 - e^{-\mu_{Si} d}) \prod_i e^{-\mu_i t_i}$$

Photon pile-up

- If ≥ 2 photons are detected by the CCD within a few pixels of each other before the frame is read-out then only one photon will be detected
- This composite photon will be recorded as having a higher energy than the two incident photons
- Leads to:
 - reduction in measured photon flux
 - “hardening” of X-ray spectra
 - distortion of point spread function
- Simple example:
 - The flux from a quasar (point source) is such that 300 photons strike a single pixel during a 200 sec observation
 - If frametime + readout-time > 1.5sec then pile-up will be important
- What are the possible solutions?

CCDs Onboard Chandra



The Advanced CCD Imaging Spectrometer (ACIS) contains 10 planar, 1024 x 1024 pixel CCDs ; four arranged in a 2x2 array (ACIS-I) used for imaging, and six arranged in a 1x6 array (ACIS-S) used either for imaging or as a grating readout.

Summary

- X-rays are collected at grazing incidence:
 - Wolter-1 configuration – confocal parabola+hyperbola
 - limits light collecting power
- Detectors are photon counting devices – Poisson limit of CCD eqn
- Proportional counters:
 - Good angular resolution, short recovery, modest energy resolution
- Micro-channel plates:
 - Great angular resolution, short recovery, modest energy resolution
- CCDs:
 - Great angular resolution, modest recovery, better energy resolution
 - Event files, not digital images transmitted back to Earth
 - Photon pile-up a concern for bright point sources